

Joint Depth and Alpha Matte Optimization via Stereo

Junlei Ma, Dianle Zhou, Chen Chen and Wei Wang

Department of Systems Engineering and Automation, National University of Defense Technology, Changsha, Hunan, China
majunlei11@nudt.edu.cn

Keywords: Stereo matching, Automatic matting, Iterative optimization.

Abstract: This study presents a novel iterative algorithm of joint depth and alpha matte optimization via stereo (JDMOS). This algorithm realizes simultaneous estimation of depth map and matting image to obtain final convergence. The depth map provides depth information to realize automatic image matting, whereas the border details generated from the image matting can refine the depth map in boundary areas. Compared with monocular matting methods, another advantage offered by JDMOS is that the image matting process is completely automatic, and the result is significantly more robust when depth information is introduced. The major contribution of JDMOS is adding image matting information to the cost function, thereby refining the depth map, especially in the scene boundary. Similarly, optimized disparity information is stitched into the matting algorithm as prior knowledge to make the foreground-background segmentation more accurate. Experimental results on Middlebury datasets demonstrate the effectiveness of JDMOS.

1 INTRODUCTION

Modern computer vision applications, such as novel view generation or z-keying require high-quality disparity maps. For these applications, producing precisely delineated disparity borders (Matsuo et al., 2015; Liu et al., 2014), which is traditionally difficult in stereo matching, is specifically important. In this study, we use the rich information near boundaries in image mattes to refine the quality of a depth map.

Image matting can be described as a labeling problem of extracting the foreground object by obtaining per-pixel opacity from its background. Basically, an image is composed of a foreground I and background B mixed with a certain degree of opacity α , which can be defined as:

$$I = \alpha F + (1 - \alpha)B \quad (1)$$

The image matting algorithm can segment the foreground and background of an image. However, Equation (1) is an ill-posed problem, because the foreground F , background B , and opacity α are unknown. Therefore, the existing matting algorithms (Levin et al., 2008; Chuang et al., 2001) require the user to first label the foreground from the background as additional constraints, which make

the matte quality deeply influenced by labeling processing. As shown in Figure 1(b), if the foreground and background specified by user is not comprehensive, the quality of matting result will be greatly degraded, compared with the red box in Figure 1(c). Figure 1(d) represents the trimap and its resulting opacity (Figure 1(e)) accurately.

Image matting can be considered as a coarse estimation of depth. Therefore, using depth is a natural way to bootstrap the process and automatically generate the trimap for image matting (Singaraju et al., 2011). The image depth can also provide new information for image matting to improve its accuracy when implementing multi-layer matting. It is a natural way to combine stereo matching algorithm and image matting algorithm to optimize each other iteratively.

The two major contributions of this study are: fusing of depth and color information to obtain high-quality fine-edge detail in the matting map and free user interaction in the matting process. The remainder of this paper is organized as follows. Section 2 is a brief summary of the state-of-the-art stereo matching and image matting algorithms. In Section 3, the algorithm framework of disparity and image matting is described, which consists of two

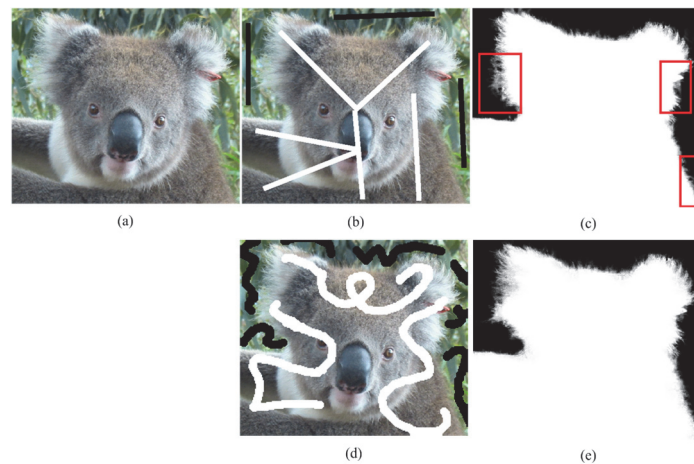


Figure 1: Human-computer interaction-based image matting. Image (a) is the original input. Image (b) is a trimap provided by users. The resulting opacity diagram of image (c) has too much noise based on image (b). Figure (d) provides another trimap by a user. Clearly, the opacity of image (e) obtained by the trimap of image (d) is more accurate.

steps: initialization and iterative optimization. We adopt a local stereo matching algorithm to generate the depth map via the opacity information. The algorithm proposed by Levin (Levin et al., 2008) is used to solve the opacity. Subsequently, we filter it with the disparity value. The experimental results in Section 4 show that the proposed algorithm is effective in disparity and image matting. A brief summary of the study and future research work are presented in Section 5.

2 RELATED WORKS

Most stereo vision disparity map algorithms have been implemented using multistage techniques. These techniques, as codified by Scharstein and Szeliski, consist of four main steps: matching cost computation, cost aggregation, disparity selection, and disparity refinement (Scharstein and Szeliski, 2002). Generally, stereo vision disparity map algorithms can be classified into local and global approaches (Hamzah et al., 2016). Local algorithms usually calculate the matching cost for a given point based on the window. Examples of implementation of such methods are provided by the work of Mattoccia et al. (Mattoccia et al., 2010), Arranz et al. (Arranz et al., 2012), Xu et al. (Xu et al., 2013), and Chen et al. (Chen et al., 2015). A representative global algorithm is the stereo matching technique via graph cuts, proposed by Boykov et al. (Boykov et al., 2001).

For the problem of image matting, the existing algorithms require the user to provide a trimap as input to distinguish the foreground and background

regions. The most widely used algorithm is the Bayesian model (Chuang et al., 2001), which transforms the matting problem into a maximum a posteriori, given the color of each pixel on the current image, and computes the maximum possible values of the foreground, background, and alpha. Wang et al. used the belief propagation to expand the local area of the sample points (Wang et al., 2007). Based on the color linear assumption, Levin et al. proposed a quadratic optimization function but only included opacity (Levin et al., 2008). Although the existing algorithms have contributed good results, most of them need interaction with the user.

Combining stereo matching and image matting algorithms can avoid user interaction. Researchers have been doing this method for a decade (Baker et al., 1998; Szeliski et al., 1998); however, the process of combining the two algorithms has a slow progress. For example, Zitnick et al. first computed the disparity map, and then used the matting algorithm according to disparity boundaries (Zitnick et al., 2004). This method relies heavily on the quality of the disparity map. Once the disparity map boundary is extracted incorrectly, this method cannot achieve the desired effect. In this study, we propose the joint depth and alpha matte optimization via stereo (JDMOS) algorithm. We do not need accurate disparity map at initialization, but only several foreground and background areas to generate the initial matting. During the iteration, the boundary details of objects in the disparity map are enhanced by combining the matting information. Consequently, the trimap region is enlarged gradually through the optimized disparity map to obtain higher quality matting.

3 ALGORITHM

Generally, without the loss, the algorithm uses the left and right images as input. These images are assumed to be rectified; thus, correspondences lie on the same horizontal scan line. Our method provides a depth map and matting information as output.

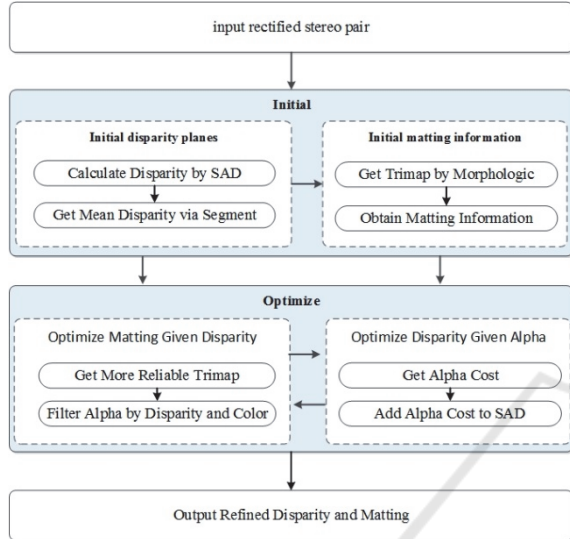


Figure 2: Overview of JDMOS.

As shown in Figure 2, JDMOS has two main phases: an initialization phase, in which an initial matte is extracted from a coarse depth; and an iterative optimization phase, in which the matte and depth are refined. In the initialization phase, the initial depth map is first generated by combining the sum of absolute differences (Tippetts et al., 2011) and the graph cut algorithm. Then, the trimap is obtained via the disparity map, and the initial opacity is calculated according to the method proposed by Levin et al. (Levin et al., 2008). During the iterative optimization stage, the opacity information of the left and right images is first added to the cost aggregation function to enhance the disparity map, especially the boundary region. The enhanced depth map is then used to provide a more reliable trimap for the matting, and the opacity is bilaterally filtered using disparity and color information. The entire optimization process is iterated until satisfactory results are obtained.

3.1 Initialization

3.1.1 Initial Disparity

First, we use the improved SAD algorithm as the cost aggregate function. The cost function is used to calculate the color distance cost C_I . The gradient distance cost C_V in the window of the size $(2n + 1) \times (2n + 1)$ for each disparity values belongs to $D = \{1, 2, \dots, d_{max}\}$, where d_{max} represents the maximum disparity ranges:

$$C_I(x, y, d) = \sum_{i=-n}^n \sum_{j=-n}^n |I_l(x+i, y+j) - I_r(x+d+i, y+j)| \quad (2)$$

$$C_V(x, y, d) = \sum_{i=-n}^n \sum_{j=-n}^n |\nabla I_l(x+i, y+j) - \nabla I_r(x+d+i, y+j)| \quad (3)$$

where x and y respectively represent the horizontal and vertical coordinates of the center point p of the window, $d \in D$; I_l and I_r represent the corresponding pixel values of the left and right images, respectively. ∇I_l and ∇I_r represent the gradient values at the corresponding points of the left and right images, respectively. Combining the color and gradient matching cost functions, we obtain the following:

$$C(x, y, d) = C_I(x, y, d) + \lambda C_V(x, y, d) \quad (4)$$

where λ is the weight that balances the effect of color and gradient information on matching costs. Experimentally, λ can be a small value.

Second, we use winner-take-all to select the optimal disparity value d_p of the pixel p ; the formula is defined as follows:

$$d_p = \arg \min_{d \in D} C(x, y, d). \quad (5)$$

Finally, we use the graph cut algorithm to segment the target image, and we obtain a series of segments $S = \{S_1, S_2, \dots, S_i, \dots, S_m\}$. The average disparity value of each pixel in the S_i is calculated as the final parallax value of the segmentation plane to remove the noise of the disparity map and enhance the disparity plane:

$$d_{S_i} = \frac{\sum_{j \in S_i} d_j}{|S_i|} \quad (6)$$

where $|S_i|$ is the number of pixels in the segment S_i .

3.1.2 Initial Matte

As shown in Figure 3, a watershed algorithm is used to divide a given depth map, binaries the segmented disparity map into foreground and background

according to the specified threshold value, then erode the foreground and background, and dilate the

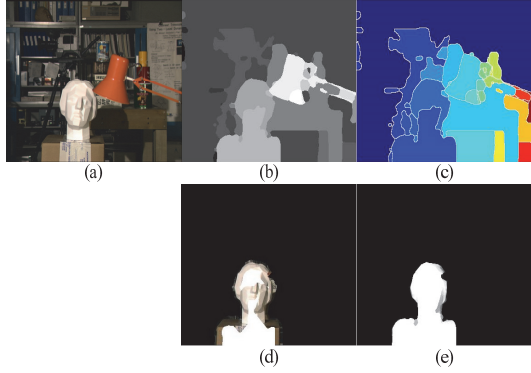


Figure 3: Initial matte. (a) Input image; (b) initialized disparity map; (c) segmentation of the initial disparity map using the watershed algorithm; (d) the trimap automatically generated by the erosion of foreground, background, and dilation of unknown regions; (e) initializing the opacity.

unknown region to generate trimap automatically. According to the method proposed by Levin et al., the basic idea is to eliminate F and B in Equation (1) based on the assumption of color linearity and obtains a quadratic optimization function (Levin, 2008):

$$J(\alpha) = \min_{\alpha, b} \alpha^T L \alpha \quad (7)$$

where L is the matting laplacian, which (i, j) th entry is

$$L(i, j) = \sum_{(i, j) \in w_k} \left(\delta_{ij} - \frac{1}{|w_k|} \left(1 + (A_i - \mu_k) \left(\sum k + \frac{\varepsilon}{|w_k I_3|} \right)^{-1} (A_j - \mu_k) \right) \right) \quad (8)$$

Here, δ_{ij} is the Kronecker delta, A_i is a 3×1 vector of the RGB for pixel in window w_k , μ_k is a 3×1 mean vector of the colors in a windows w_k , $\sum k$ is a 3×3 covariance matrix, $|w_k|$ is the number of pixels in this window, and I_3 is the 3×3 identity matrix.

3.2 Optimization

In this section, we apply a two-step procedure. First, given the opacity, add the opacity consistency of the left and right images to the cost aggregation function to enhance the disparity map. Second, given the optimized disparity map, obtain more reliable trimap and filter opacity to refine mattes. These two steps are iterated, and results show that the proposed

algorithm can achieve satisfactory results with only two to three iterative steps.

3.2.1 Optimize Disparity Plane

The opacity information of the left and right images is obtained. Subsequently, similar method is applied in the window of size $(2n + 1) \times (2n + 1)$ for each disparity value that belongs to $D = \{1, 2, \dots, d_{\max}\}$, where d_{\max} represents the maximum parallax range. We use C_α to measure the matching cost of the left and right opacities:

$$C_\alpha(x, y, d) = \sum_{i=-n}^n \sum_{j=-n}^n |\alpha_l(x + i, y + j) - \alpha_r(x + d + i, y + j)| \quad (9)$$

where α_l and α_r represent the opacity of the corresponding pixel of the left and right images, respectively.

C_α is added to Equation (4); then, the optimized cost aggregation function C' is obtained as follows:

$$C'(x, y, d) = C(x, y, d) + \xi C_\alpha(x, y, d) \quad (10)$$

where ξ is the balance parameters.

3.2.2 Optimize Matte

Given the optimized disparity map, we use the watershed segmentation. When generating the trimap, we can narrow the uncertain region by reducing the erode/dilation band size around 2–4 pixels.

The disparity value is added as the 4th channel with the original R, G, and B channels for a color image, and the A_i in Equation (8) is modified to combine RGB with disparity D to fully utilize the optimized disparity information and enhance the matting effect (Zhu et al., 2009).

Although Zhu et al. added weight to the disparity value (Zhu et al., 2009); the basic assumptions of Levin et al. regarding color linear assumption are disproved. Figure 4(c) shows the RGB value distribution of all the pixels in a small window and verifies the correctness of the color linearity assumption. Figures 4(d), 4(e), and 4(f) can be used as the projection of the RGBD values of all the pixels in the small window on R, G, and B and show that the values of the pixels in a small window do not lie on a single line in the RGBD space, especially at the boundaries of the disparity variation.

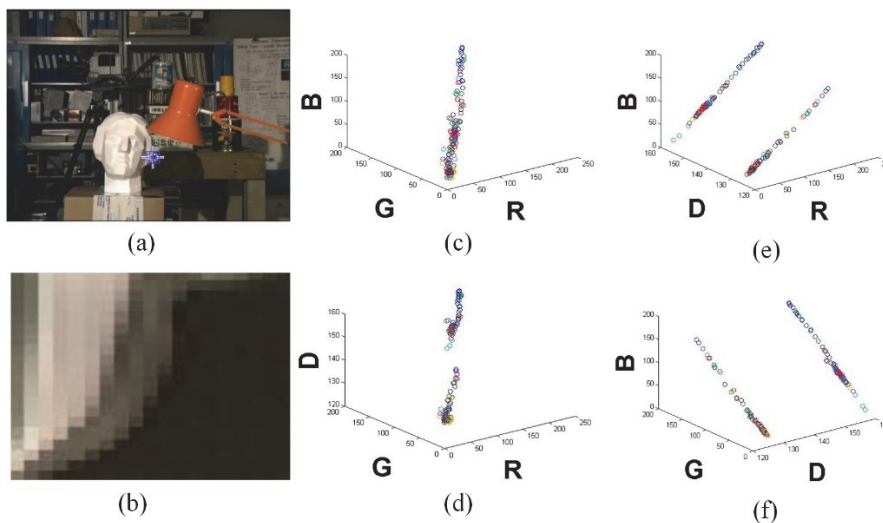


Figure 4: Distribution of pixels within a small window: (a) Original image; (b) a small window selected from image (a); (c) distribution of the RGB distribution of all the pixels in window (b); (d) distribution of the RGD of all the pixels in window (b); (e) distribution of the RBD values for all the pixels in window (b); (f) distribution of the GBD values for all the pixels in windows (b). Images (c), (d), (e), and (f) can also be viewed as the projections of the RGBD values of all the pixels in window (b) on D, B, G, and R, respectively.

Therefore, we propose a method to weigh the opacity obtained via the method (Levin et al., 2008) using the disparity and color information. Evidently, if the disparity values of the two pixels are significantly different, then these are likely to belong to different layers and the weight becomes smaller. If the colors of the two pixels are similar, the weight value will increase accordingly. After filtering, the opacity of pixel i become:

$$\alpha_i = \frac{\sum_{j \in W(i)} W_C(I(i), I(j)) \cdot W_D(d(i), d(j)) \cdot \alpha(j)}{\sum_{j \in W(i)} W_C(I(i), I(j)) \cdot W_D(d(i), d(j))} \quad (11)$$

where W_C and W_D denote the weights of color and disparity distances, respectively, which are defined as follows:

$$W_C(I(i), I(j)) = \exp\left\{-\left\|\frac{I_i - I_j}{w_c}\right\|^2\right\} \quad (12)$$

$$W_D(I(i), I(j)) = \exp\left\{-\left\|\frac{d_i - d_j}{w_d}\right\|^2\right\} \quad (13)$$

where w_c and w_d are used to adjust the weight of the color and distance of disparity value, respectively.

4 EXPERIMENTS

We evaluate JDMOS using the Middlebury dataset. The parameters in Equations (4) and (10) are set to the constant values of $\lambda = 0.8$ and $\xi = 0.5$. With CPU at 2.00 GHz, it takes approximately 20 s to process an image size of 384×288 averagely.

4.1 Optimized Result

By applying the methods in the initialization and optimization phases, we compare the disparity map and matting before and after optimization. The experimental results on Tsukuba are shown in Figure 5. On the initial depth map (e), several abnormal points (black holes) are present on the left side of the paper box, and several noise spots appear in the initial mattes (c). After two iterations, the depth map (f) is enhanced at the boundaries because of the increase in matting information. Similarly, since the depth of information is incorporated into the image matting algorithm, mattes (b) have also been significantly improved in the foreground and background layers. The entire experiment process is automated without human interaction. More results on Kid are shown in Figure 6.

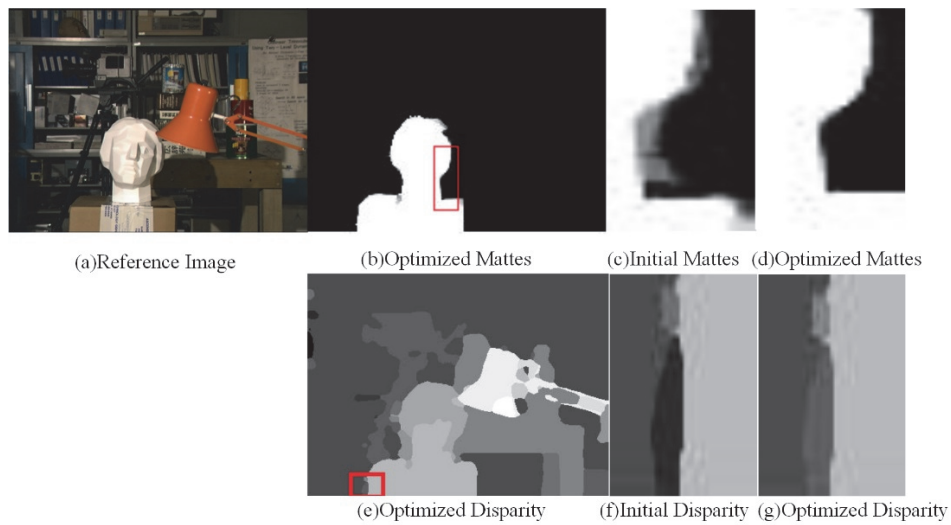


Figure 5: Experiment results of the algorithm on the Tsukuba image.

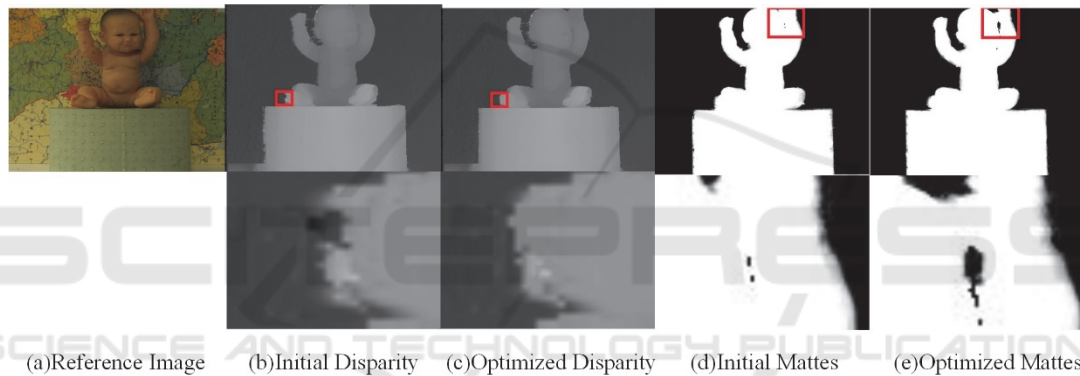


Figure 6: More results from the Kid image.

4.2 Algorithm Robustness

We compare the method proposed by Levin (Levin, 2008) as manual matting with JDMOS. As shown in Figure 7, manual matting has poor performance in some cases, in which the input of the user's input is not representative. Conversely, our algorithm is relatively robust.

The quality of the manual matting is heavily dependent on the input of the user. Figures 7(a) and 7(e) are two different user inputs. The information provided in Figure 7(e) is more comprehensive, making the result more accurate, as shown in Figure 7(f). For Figure 6(a), the area between the face and arm of the baby is only a few pixels away (Figure 7(a) at the red frame). Marking a certain background information between them is difficult for the user.

Therefore, neither of the two types of manual matting distinguishes the area correctly, as shown in Figures 7(d) and 7(h). In contrast, our algorithm does not rely on human manipulation, thereby resulting in more robust image matting; Figure 7(n) further proves that the proposed algorithm can solve the problem mentioned above by integrating the disparity information into the image matting based on the ground truth.

5 CONCLUSION

In this study, given the complementary nature of alpha matte and depth, an iterative feedback method is presented to enhance their quality mutually.

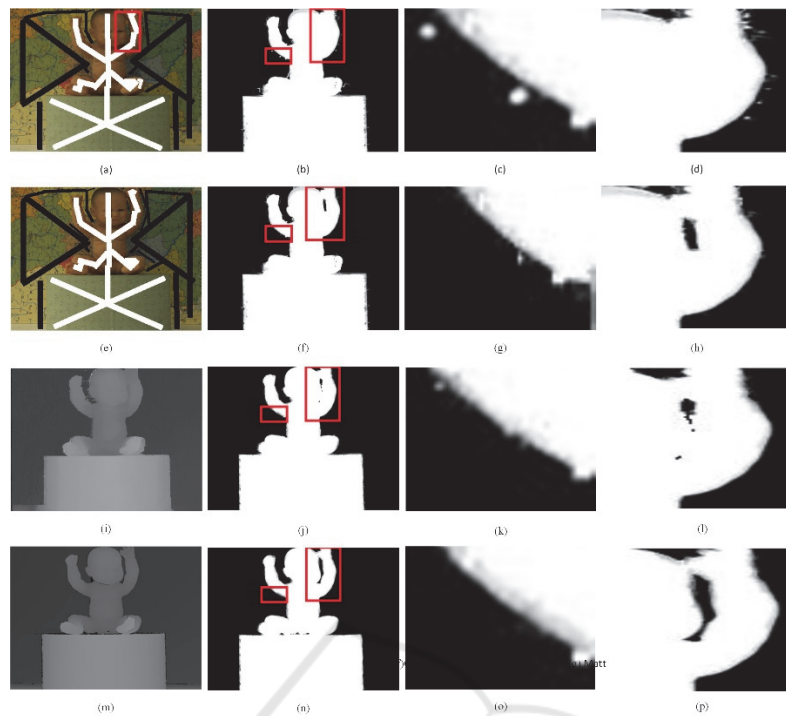


Figure 7: Comparison among JDMOS, manual matting, and matting via ground truth. Image (a) is a user input; (b) is the opacity obtained by (a) as a trimap; (c) and (d) are enlarged views of the red frame in (b); (e) is another user input; (f) is the opacity obtained by (e) as a trimap; (g) and (h) are enlarged views of the red frame in (f); (i) is the disparity map after optimization; (j) is the opacity obtained via (i); (k) and (l) are enlarged views of the red box in (j); (m) is the ground truth; (n) is the opacity obtained by (m); and (o) and (p) are enlarged views of the red box in (n).

Compared with manual matting, our proposed algorithm is free from human interaction, which avoids uncertainty generated from user operations and can handle what humans cannot address. For example, the area between foreground and background is extremely narrow that users cannot mark on it. Experiments show that JDMOS is robust to a few difficult situations and can reduce the error of the disparity map and improve the accuracy of the image matting.

The matting problem is under-constrained and intrinsically difficult. JDMOS has made some important advancement in this problem; however, one limitation remains to be addressed. The quality of the result is partly dependent on the quality of the initial depth map.

In the following study, we will focus on the improvement of the optimization function. We expect to combine binocular stereo matching with the image matting algorithm using only one energy optimization function to fuse the two information more closely. Also, we are interested in editing multiple regions in an image.

REFERENCES

- A. Levin, D. Lischinski, and Y. Weiss. 2008. A closed form solution to natural image matting. *IEEE Trans. on PAMI*, 30(2): 228–242.
- Y. Chuang, B. Curless, D. Salesin, and R. Szeliski. 2001. A Bayesian approach to digital matting. In *CVPR (2)*, pages 264–271, 2001.
- D. Scharstein and R. Szeliski. 2002. A taxonomy and evaluation of dense two-frame stereo correspondence algorithms. *International Journal of Computer Vision*, vol. 47, no. 1–3, pp. 7–42.
- S. Mattoccia, S. Giardino, and A. Gambini. 2010. Accurate and efficient cost aggregation strategy for stereo correspondence based on approximated joint bilateral filtering. In *Proceedings of the Asian Conference on Computer Vision (ACCV '10)*, vol. 38, pp. 371–380, Xi'an, China.
- L. Xu, O. C. Au, W. Sun et al., 2013. Stereo matching by adaptive weighting selection based cost aggregation. in *Proceedings of the IEEE International Symposium on Circuits and Systems (ISCAS'13)*, pp. 1420–1423, Beijing, China.

- A. Arranz, A. Sánchez, and M. Alvar. 2012. Multi resolution energy minimisation framework for stereo matching. *IET Computer Vision*, vol. 6, no. 5, pp. 425–434.
- Y. Boykov, O. Veksler, R. Zabini. 2001. Fast Approximate Energy Minimization via Graph Cuts [J], *IEEE Trans. on PAMI*, 23(1):1222-1239.
- J. Wang and M. Cohen. 2007. Simultaneous matting and compositing. In *CVPR*.
- S. Baker, R. Szeliski, and P. Anandan. 1998. A layered approach to stereo reconstruction. In *CVPR*, pages 434–441.
- R. Szeliski and P. Golland. 1998. Stereo matching with transparency and matting. In *ICCV*, pages 517–525.
- L. Zitnick, S. Kang, M. Uyttendaele, S. Winder, and R. Szeliski. 2004. High-quality video view interpolation using a layered representation. *ACM Transaction on Graphics*, 23(3):600–608.
- Ruigang Yang, Jiejie Zhu, Miao Liao, Zhigeng Pan. 2013. Joint depth and alpha matte optimization via fusion of stereo and time-of-flight sensor. *IEEE Conference on Computer Vision and Pattern Recognition*, vol. 00, no. , pp. 453-460, 2009,
- T. Matsuo, S. Fujita, N. Fukushima, and Y. Ishibashi. 2015. Efficient edge-awareness propagation via single-map filtering for edge-preserving stereo matching, in *Three-Dimensional Image Processing, Measurement (3DIPM), and Applications*, vol. 9393 of *Proceedings of SPIE, International Society for Optics and Photonics*, San Francisco, Calif, USA.
- J. Liu, X. Sang, C. Jia, N. Guo, Y. Liu, and G. Shi. 2014. Efficient stereo matching algorithm with edge-detecting, in *Optoelectronic Imaging and Multimedia Technology III*, vol. 9273 of *Proceedings of SPIE*, p. 7.
- B. J. Tippetts, D.-J. Lee, J. K. Archibald, and K. D. Lillywhite. 2011. Dense disparity real-time stereo vision algorithm for resource limited systems, *IEEE Transactions on Circuits and Systems for Video Technology*, vol. 21, no. 10, pp. 1547 - 1555.
- D. Chen, M. Ardabilian, and L. Chen. 2015. A fast trilateral filter based adaptive support weight method for stereo matching, *IEEE Transactions on Circuits and Systems for Video Technology*, vol. 25, no. 5, pp. 730 - 743.
- Rostam Affendi Hamzah and Haidi Ibrahim. 2016. Literature Survey on Stereo Vision Disparity Map Algorithms. *Journal of Sensors*, vol. 2016, Article ID 8742920, 23 pages, doi:10.1155/2016/8742920.
- Dheeraj Singaraju, Rene Vidal. 2011. Estimation of Alpha Mattes for Multiple Image Layers, *IEEE Transactions on Pattern Analysis and Machine Intelligence*, v.33 n.7, p.1295-130